Interplay between electronic structure and surface phase transition on α-Ga(010)

Ch. Søndergaard, Ch. Schultz, S. Agergaard, S. V. Hoffmann, Z. Li, and Ph. Hofmann
Institute for Storage Ring Facilities, University of Aarhus, 8000 Aarhus C, Denmark

H. Li
Institute for Storage Ring Facilities, University of Aarhus, 8000 Aarhus C, Denmark
and Department of Physics, Zhejiang University, Hangzhou 310027, China

Ch. Grütter and J. H. Bilgram
Laboratorium für Festkörperphysik, Eidgenössische Technische Hochschule, 8093 Zürich, Switzerland
(Received 10 April 2002; revised manuscript received 21 October 2002; published 29 April 2003)

The interplay between the surface phase transition on α-Ga(010) and the electronic structure was studied by temperature-dependent high-resolution angle-resolved photoemission using synchrotron radiation. The transition causes several changes in the spectral features. Most importantly, it is accompanied by a decrease of spectral intensity around the Fermi level in large fractions of the surface Brillouin zone. Moreover, it leads to a quasidiscontinuous change in the temperature-dependent linewidth of the dangling-bond surface state at $\overline{C}$. Finally, an electronic state was observed in the low-temperature phase very close to the Fermi level at $\overline{C}$. We discuss these findings in the context of a surface charge-density wave model. Above the transition temperature, the electronic structure is somewhat reminiscent of the low-temperature phase but it is influenced by strong fluctuations.

DOI: 10.1103/PhysRevB.67.165422 PACS number(s): 73.20.−r, 68.35.−p, 63.20.Kr

I. INTRODUCTION

The stable α phase of gallium is a metal with an unusual structure and a number of intriguing properties. The bulk structure is face-centered orthorhombic with eight atoms per unit cell.[1] Each atom has only one nearest neighbor such that the structure can be viewed as being made of Ga_2 dimers or ''molecules'' (see Fig. 1). The covalent and localized bonding character of the dimers is also reflected in the electronic structure where it leads to rather flat bands in certain directions of k space.[2,3] Metallicity is only present in the so-called buckled planes where the ends of the dimers overlap. This gives rise to a very anisotropic Fermi surface[2] and corresponding transport properties. Moreover, α-Ga has an unusually low melting temperature of only 303 K. As might be expected from the structure, the electron-phonon interaction plays an important role in bulk α-Ga. The upper limit for the phonon frequencies is 40 meV,[4] and the electron-phonon mass enhancement parameter λ has a value of 0.98.[5]

The properties of the α-Ga(010) surface[28] have so far been studied by optical techniques,[6] scanning-tunneling microscopy (STM),[7,8] x-ray diffraction,[9] low-energy electron diffraction (LEED),[10] spot profile analysis (SPA) LEED,[11] angle-resolved photoemission spectroscopy (ARPES),[12] and first-principles calculations.[13] Several interesting properties have been found, among others an extraordinary thermal stability. The surface appears to be stable up to[6] and even beyond[8] the bulk melting point. Furthermore it has been found that the electron-phonon coupling on the surface is very strong, even stronger than in the bulk[12] and finally that the surface undergoes a reversible phase transition upon cooling below 220 K.[12] Understanding the nature of this phase transition and its interplay with the electronic structure is the main objective of this paper.

A. Structural properties

The [010] direction is almost parallel to the direction of the dimers in the bulk, and for the (010) surface one can imagine two possible terminations of the bulk structure. The so-called A termination is a configuration where the crystal is cleaved without cutting the interdimer bonds. In the B termination these bonds are cut, creating dangling bonds at the surface and a metallic surface state.[13] Both terminations are indicated in Fig. 1. In addition to these bulk terminations, a third structural model, the C termination, has been proposed by Bernasconi, Chiarotti, and Tosatti (BCT).[13] It consists of a reconstruction with (1×1) periodicity which can be thought of as two layers of Ga III, another bulk modification, covering the (010) surface of α-Ga. In BCT's calculations, the C model had the lowest total energy and this was found to explain the thermal stability.[13] Figure 2 shows the top view of α-Ga which is identical for all three suggested surface terminations: it is a rectangular (almost-square) unit cell containing two atoms, one at the corners and one slightly moved off the center. For all three terminations one would expect to observe a LEED pattern in which every odd-integer spot in the [100] direction is missing because of the glide-plane symmetry of bulk α-Ga which is preserved in the surface structure.

Atomically resolved STM images taken near the melting temperature by Züger and Dürig[7] show the expected structure but due to the lack of depth sensitivity in STM they do not reveal which termination is actually present. However, only steps of height $c/2\approx3.8$ Å are observed indicating that only one termination prevails on the surface. It has to be noted that the STM data also give some indications of a possible surface reconstruction in which the atom near the center of the unit cell is moved slightly off its ideal position

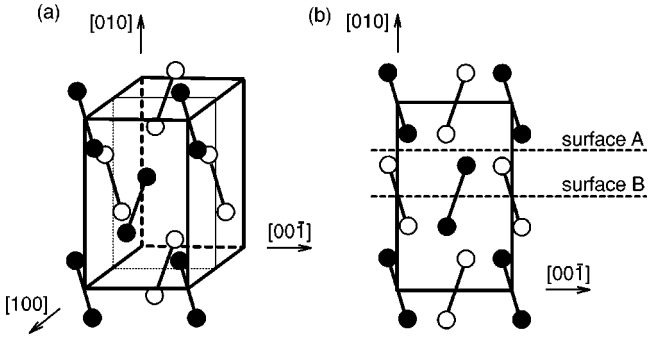

FIG. 1. (a) The α-Ga crystal structure with the Ga_2 dimers emphasized. (b) Side view where the two possible truncated-bulk surfaces A and B are indicated.

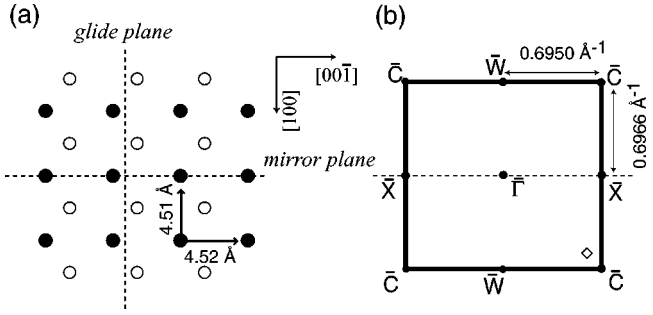

FIG. 2. (a) Top view of α-Ga(010). Only the first layer is shown. This first layer geometry is identical for the terminations in Fig. 1. (b) Surface Brillouin zone of α-Ga(010). The marker ($\diamond$) between $\bar{\Gamma}$ and $\bar{C}$ indicates the $\vec{k}_{\parallel}$ point where the data in Fig. 11 below were taken.

towards one of the corner atoms.[7] Such a reconstruction breaks the glide-plane symmetry and is consistent with the fact that Züger and Dürig have observed a (1×1) LEED pattern with no missing spots. A broken glide-plane symmetry has also been found by Walko *et al.*[9] in a surface x-ray-diffraction study pointing towards a B termination.

Dedicated LEED experiments, however, observe a glide-plane symmetry in accordance with the suggested surface terminations. LEED (Ref. 10) and SPA-LEED (Ref. 11) studies observe the expected missing spots on well-aligned[29] surfaces near the melting temperature. A quantitative LEED analysis finds the surface to be a relaxed type-B bulk termination.[10]

An ARPES study by Hofmann, Cai, Grütter, and Bilgram[12] (HCGB) yielded an electronic structure which resembles the theoretical result of the B termination.[13] A predicted surface state was found at the $\bar{C}$ point of the surface Brillouin zone (SBZ) and the surface states in the lower-lying gaps which are predicted only for the A (Ref. 14) and the C (Ref. 13) terminations were indeed not observed. There were, however, two noteworthy points of disagreement. First, from the theoretical result an almost circular surface Fermi surface around the $\bar{C}$ point is expected.[13] This did not seem to be the case in the experiment, even though HCGB did not systematically measure the Fermi surface. Second, a predicted surface state near the $\bar{\Gamma}$ point could not be observed. In the present work we have now been able to find this state. In conclusion, it is a well-established fact that in the high-temperature (HT) phase, close to the melting temperature, the surface structure is a relaxed type-B bulk termination.

B. Low-temperature phase

HCGB have observed that the surface undergoes a reversible phase transition at about 220 K.[12] Above this temperature the LEED pattern is (1×1) with missing spots. Upon cooling below approximately 220 K the LEED pattern changes reversibly from (1×1) to $c(2\times2)$ or $(\sqrt{2}\times\sqrt{2})R45°$ in the low-temperature (LT) phase. Later additional spots have been found in the LT LEED pattern.[10] These spots are very weak and only observable in a small energy window. However, it turns out that the correct description of the LT LEED pattern is $(2\sqrt{2}\times\sqrt{2})R45°$. To make matters even more complicated, SPA-LEED has shown that the overstructure spots in the LT phase are actually split along the direction of the glide plane by a very small amount, corresponding to a real-space distance about 18 times larger than the (1×1) unit cell.[11]

Using dynamic LEED analysis Moré and co-workers have not only been able to determine the structure of the (1×1) phase but also that of the low-temperature phase.[10] As mentioned above, the high-temperature phase is a relaxed form of the B termination. Good agreement between measured and simulated LEED $I(V)$ curves could be achieved but only by assuming a very low surface Debye temperature. This indicates the presence of large-amplitude thermal vibrations or other types of disorder. The LT structure can be obtained from the HT structure by shifting the surface atoms, since no major mass transport is involved. There is a certain degree of dimerization, likely to remove some of the dangling bonds present on a B-terminated (1×1) phase. As for the HT structure, a low surface Debye temperature has to be assumed in order to achieve good agreement between experiment and simulations.

C. Surface phase transition

The aim of the present work is to study the detailed interplay between the surface electronic structure and the phase transition in order to find the driving force behind the reconstruction. The above-described behavior is complicated, however, there are some facts which do point towards a possible scenario for a phase transition. From energetic grounds, a B termination of the surface does not seem to be very favorable because the bonds between the surface dimers need to be broken, leaving a crystal which is terminated with a buckled plane and which supports a high density of dangling bonds. One could expect this surface to undergo a metal-insulator transition, removing the dangling bonds, or at least a fraction of them, by dimerization, a picture which seems consistent with the LEED results for the LT phase. A surface metal-insulator transition should be identifiable in the electronic structure, in particular, in the states very close to the Fermi level. Apart from the removal of dangling bonds, other mechanisms might contribute to the phase transition, in particular, the strong electron-phonon coupling.

A type of surface metal-insulator transition which has recently attracted considerable attention is the formation of a charge-density wave (CDW). While this type of instability is most likely to occur in one-dimensional systems,[15] it has also been observed in quasi-two-dimensional crystals such as the transition-metal dichalcogenides as well as on clean and adsorbate-covered surfaces.[16,17] The main idea behind a CDW can be explained as follows. One introduces a periodic lattice distortion in a normal metal. This distortion will give rise to a new Brillouin zone with gaps in the band structure opening at the zone boundaries. If the new zone boundaries coincide with large ''nested'' parts of the original Fermi surface, the energy of many occupied states will be decreased by the opening of the gaps. If this electronic energy gain is larger than the elastic energy which has to be spent to create the distortion, the new CDW ground state is stable. In principle, this type of phase transition should be easily found in photoemission: in the HT metallic phase one should be able to observe the nested Fermi surface which disappears by opening a gap in the LT phase.

Unfortunately, the general situation is never this clear cut. The properties of the system depend on the strength of the electron-phonon coupling and Tosatti has introduced a convenient distinction between ''weak-'' and ''strong-'' coupling CDW scenarios.[16] In a strong-coupling CDW material the electronic states can be changed in a large fraction of the SBZ and the gap can be much larger than in the weak-coupling case described above.[18,19] Moreover, the phase transition from the ordered CDW phase to the HT phase is strongly influenced by fluctuations. Just above the transition temperature the long-range order which characterizes the CDW state is lost but short-range order of a similar nature may still be present and lead to confusing photoemission results

The present paper is structured as follows: after this introduction we describe the experimental procedures. Handling and cleaning α-Ga is not an easy task because of the low melting temperature and there is a risk that experimental results become history dependent. Therefore we report some details which are usually omitted for more ''normal'' metals. In the results section we first give an overview of the different surface electronic states. After this, we describe the temperature dependence of some of these states, of the surface Fermi surface and of the Ga $3d$ core levels. This is followed by a detailed discussion and a short section giving the main conclusions of our work.

II. EXPERIMENT

The photoemission experiments were performed using an angle-resolved electron spectrometer at the SGM-3 beamline on the undulator of the storage ring ASTRID in Aarhus. A detailed description of the instrument is given elsewhere.[20] In short, the beamline covers an energy range from 13 eV to 130 eV with a resolving power better than 15 000. Alternatively, data can be taken using unpolarized He I radiation from a UV lamp. The electron spectrometer is a commercial hemispherical analyzer (VG-ARUPS10) which is mounted on a goniometer inside the chamber and equipped with a multichannel detector. The analyzer position can be changed by motors outside the chamber. The total-energy resolution used in this work was around 40 meV. The angular resolution was approximately $\pm 0.7°$. The pressure during the experiments with synchrotron radiation was in the 10^{-11}-mbar range. Samples could be mounted on the end of a closed-cycle He refrigerator and cooled down to approximately 30 K. The temperature was monitored via a K-type thermocouple. If measurements were to be performed above 30 K, this had to be done by heating the sample using radiative heat from a filament behind the sample holder. The filament current could either be pulsed as to avoid a possible influence of the magnetic field on the measurement or it could be turned on continuously. We decided to perform the temperature-dependent measurements in the latter mode after having carefully tested that the influence of the magnetic field on our results was negligible. Most spectra were obtained at photon energies of 15.5, 17.0, and 24.5 eV. These energies are not special but are good choices in the sense that the investigated surface electronic states are well separated from bulk peaks and have relatively high intensities.

Our α-Ga(010) sample was mechanically polished to a perfect mirror finish. After insertion into the vacuum system via a load-lock the surface was cleaned by sputtering with 0.5–2.0 keV Ne^+ ions and ''annealing'' between 253 K and 273 K. This procedure resulted in a sharp (1×1) low-energy electron-diffraction (LEED) pattern at 273 K. Every odd-integer spot in the [100] direction was missing, consistent with bulk glide-plane symmetry. Surface cleanliness was checked by photoemission. In the initial stages of the cleaning, monitoring the oxygen peaks in the valence band proved useful. Once an almost clean surface was obtained, the spectral shape of the surface state at $\bar{C}$ was found to be a more sensitive measure of the surface quality. As we show later, some spread was found in the surface-state linewidth at a certain temperature following a given combination of sputtering and annealing. The reason for this is most likely due to the preparation history. It is, for example, conceivable that if the surface is ''annealed'' close to room temperature for a long time, then one may obtain a narrower linewidth after the cleaning procedure. Although a systematic history dependence could not be established, we believe that the limitations of an effective high-temperature annealing of this surface affect the observed spread in linewidth.

The temperature scans were performed using two different approaches. The first was to clean the sample at 273 K and to cool it down slowly, taking the data at the desired temperatures. Cooling down the cryostat from 273 K to 30 K takes about one hour plus the time needed to collect the data. This method works very well for temperatures above 80 K where the surface is rather insensitive to contamination. At lower temperatures the surface was found to be more reactive. At 30 K the quality of the surface states decays quickly, and spurious peaks become visible in the spectrum.[21] The other approach also involved cleaning the sample at 273 K. Then, however, it was taken out of the cryostat and left on a wobble stick at room temperature until the cryostat was cooled down. Subsequently it was inserted again and cooled

to 30 K within a few minutes. The data were taken by warming the sample in steps.

For the photoemission measurements the sample was positioned such that the angle between the surface normal and the incident light was 40° and 60° for the measurements with synchrotron radiation and He *I*, respectively. The azimuthal orientation of the sample was chosen such that the polarization vector of the synchrotron radiation was oriented along the $\overline{\Gamma}$-$\overline{C}$ direction of the SBZ.

All spectra taken with synchrotron radiation were normalized to the photoemission current of the last focusing mirror in the beamline. This enabled us to compare the absolute count rates, for example, for a set of temperature-dependent spectra.

III. RESULTS

A. Surface electronic structure: An overview

As mentioned above, the surface electronic structure of α-Ga(010) as determined here and previously in Ref. 12 resembles closely the theoretical result obtained by BCT for the relaxed B termination.[13] We found a surface state situated in the projected band gap around the $\overline{C}$ point of the SBZ. The experimental binding energy of this state at the high-symmetry point was around 1.1 eV and thus somewhat larger than the calculated value of 0.5 eV. This surface state is a dangling-bond state which arises due to the cutting of the dimers. It is doubly degenerate since each of the two atoms in the surface unit cell supports such a state. We call this state the S_H state in the following. Its dispersion, Fermi surface and temperature dependence is discussed in detail below.

BCT's theoretical results for the A and C terminations[13,14] predict surface states in the lower-lying projected band gaps which have a binding energy between 6 and 9 eV. Such states could not be found, neither by HCGB,[12] nor us.

BCT also predicted a surface state at the $\overline{\Gamma}$ point of the SBZ for all three terminations. This state was not observed by HCBG but we have found it in the present work. It is shown in Fig. 3. Its binding energy is about 0.5 eV, consistent with the theoretical prediction.[13] The state was identified by its position in a projected bulk band gap and the fact that its binding energy is not altered upon a change of $k_\perp$ via the photon energy.[3] The reason why the state was not observed by HCBG was the limited temperature and photon energy range in that work. At low energies and high temperatures the state is only visible as a very weak shoulder and is therefore not easily recognized. The weak cross section for this surface state and its proximity to the bulk continuum make it a poor candidate for studying temperature dependence and this was not attempted.

Finally, a second surface-related feature was found at $\overline{C}$ very close to the Fermi energy for the LT structure. We call it the S_L state in the following. Such a state is not predicted for any of the three bulk terminations considered by BCT. The state has already been observed by HCBG as a weak shoulder.

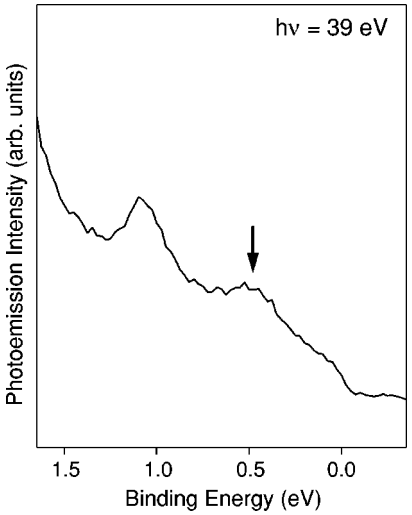

FIG. 3. Energy distribution curve (EDC) taken in normal emission at $T=78$ K. The small feature at about 0.5-eV binding energy is the surface state at the $\overline{\Gamma}$ point in the surface Brillouin zone.

B. The two surface states at $\overline{C}$

Two surface states can be found at $\overline{C}$. The first is the dangling-bond state S_H with a binding energy of about 1.1 eV which can be observed at all temperatures. The second is the additional state S_L found at low temperatures and very close to the Fermi level. Spectra of the low-temperature electronic structure at $\overline{C}$ taken at two different photon energies are shown in Fig. 4. The figure illustrates the independence of the features from $k_\perp$. Both spectra have been taken such that the S_H surface state is exactly at $\overline{C}$, and the S_L state is not. Moving the analyzer to the angle at which the S_L state is at $\overline{C}$ leads to an intensity increase in that peak. It is very difficult to make statements about the binding energy and width of the S_L state since it appears to be cut off by the

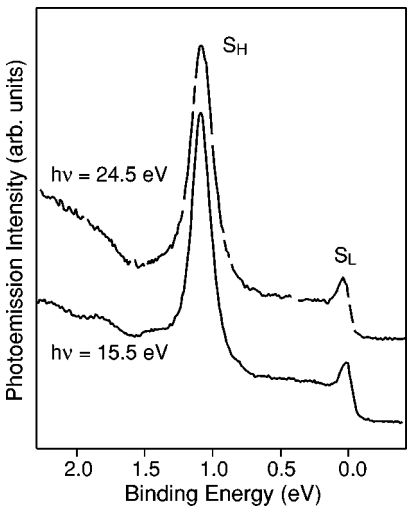

FIG. 4. EDC's taken at $T=45$ K for two different photon energies with the S_H surface state at $\overline{C}$. The S_L surface state is only approximately at $\overline{C}$.

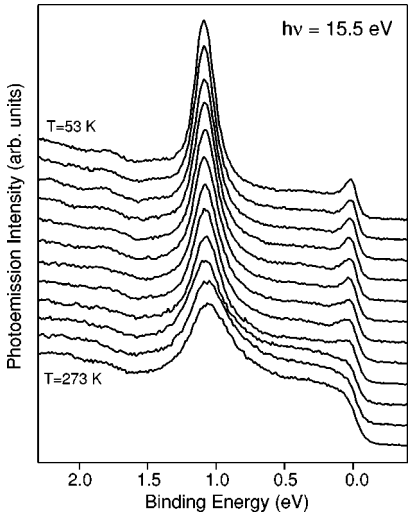

FIG. 5. Temperature dependence of the surface electronic structure at $\bar{C}$. The spectra have been normalized by the photoemission current of the last beamline mirror and are plotted with a constant offset. The temperature is changed by $\Delta T = 20$ K between the spectra.

Fermi level. At the lowest temperatures the S_L state is very sensitive to surface contaminations.

Figure 5 shows a typical set of energy distribution curves (EDC's) taken with the S_H state at the $\bar{C}$ point as a function of temperature. One clearly observes the narrowing of the S_H peak and the evolution of the S_L peak as the temperature is lowered. An interesting spectral feature is the high background intensity between the surface state and the Fermi level. From the gap in the bulk band structure one would actually expect the spectral intensity to be zero or at least very low. Finite intensities can be created by scattering events which change the electron energy not at all or only very little, notably events such as phonon or impurity scattering. At least at the lowest temperatures phonon scattering is unimportant. It is also inconceivable to assume a high amount of defects for this surface since the methods of preparation used here are known to lead to highly ordered surfaces with very large terraces.[8,11]

The temperature dependence of a surface-state linewidth can be used to extract information about the strength of the electron-phonon coupling on the surface as expressed by the so-called electron-phonon mass enhancement parameter λ.[22] In short, this type of analysis is based on the following assumptions. The linewidth of the surface-state peak is directly connected to the inverse lifetime of the valence hole by $\Gamma_h = 2\pi/\tau$. There are three independent contributions to the lifetime: $\Gamma_h = \Gamma_{e\text{-}e} + \Gamma_{e\text{-}i} + \Gamma_{e\text{-}ph}$. The first, $\Gamma_{e\text{-}e}$, is Auger decay via the electron-electron interaction. The second, $\Gamma_{e\text{-}i}$, is defect or impurity scattering which elastically scatters the hole, and the third, Γ_{e-ph}, is phonon scattering. The two first effects may give a considerable contribution to the hole lifetime but it is fair to assume that their temperature dependence is small. This leaves the electron-phonon interaction as the major contribution to the temperature dependence. The inverse lifetime due to this interaction is given by

$$\Gamma_{e\text{-}ph} = 2\pi\hbar \int_0^{\omega_{max}} d\omega' \alpha^2 F(\omega')[1 - f(\omega - \omega') + 2n(\omega') + f(\omega + \omega')], \quad (1)$$

where $\alpha^2 F(\omega)$ is the Eliashberg coupling function, $f(\omega)$ and $n(\omega)$ are the Bose and Fermi distributions, respectively, and ω_{max} is the maximum phonon frequency. The Eliashberg coupling function contains the phonon spectrum and can be approximated in the Debye model as $\alpha^2 F(\omega) = \lambda(\omega/\omega_D)^2$ for $\omega < \omega_D$ and zero elsewhere;[5] ω_D is the Debye frequency. In the limit of high temperature, $T > \omega_D/3$, and energies close to the Fermi energy, a simple linear approximation to Eq. (1) is valid:

$$\Gamma_{e-ph} = 2\pi\lambda kT. \quad (2)$$

The Debye approximation is actually a three-dimensional scheme, but calculations show that surface effects only give rise to small corrections, and the use of the Debye spectrum is not expected to be a large source of errors either.[23] In the case of Ga with its low melting point Eq. (2) is only applicable in a limited temperature range. Therefore we also analyze the data with Eq. (1) assuming the Debye approximation to the Eliashberg coupling function. In both cases a temperature-independent offset, Γ_0, due to electron-electron and electron-impurity scattering, is added to $\Gamma_{e\text{-}ph}$.

An additional point to consider is how the measured linewidth, Γ_m, is related to the hole-state linewidth Γ_h. A surface state has no dispersion with $k_\perp$ and in this case

$$\Gamma_m = \frac{\Gamma_h}{\left|1 - \frac{m v_{h\parallel} \sin^2\theta}{\hbar k_\parallel}\right|}, \quad (3)$$

where θ is the emission angle and $v_{h\parallel}$ is the group velocity, $v = \hbar^{-1}\partial E/\partial k_\parallel$.[24,25] In this experiment the emission angle is chosen such that the surface state is exactly at the symmetry point $\bar{C}$, then $v_{h\parallel} = 0$ and Eq. (3) reduces to $\Gamma_m = \Gamma_h$.

For a quantitative analysis of the line shape, we proceed as demonstrated in Fig. 6, and fit a Lorentzian-like line shape to the peak in order to obtain the inverse lifetime of the hole state. The peak is slightly asymmetric and not purely Lorentzian due to the angular resolution of the analyzer (and any other $k_\parallel$-integrating mechanisms). However, the high binding-energy side of the peak ought not to be broadened since the surface state is at an extremum of maximum binding energy, and hence only states with less binding energy can be scattered into the emission direction by an integration over $k_\parallel$. For this reason we approximate the peak shape with a line shape consisting of two "half" Lorentzians. The part of the peak below the binding energy is a Lorentzian with width $\Gamma_<$ while the other part has width $\Gamma_>$. The full width at half maximum of the peak is then $\Gamma = 1/2 \cdot (\Gamma_< + \Gamma_>)$. We use $\Gamma_m = 2\Gamma_<$ as the best measure of the inverse hole-state lifetime. Note that this way of fitting allows us to quantify the asymmetry, $\alpha = (\Gamma_> - \Gamma_<)/(\Gamma_> + \Gamma_<)$, and to see if it depends on temperature. Our fits show no systematic temperature dependence of the asymmetry and we obtain an

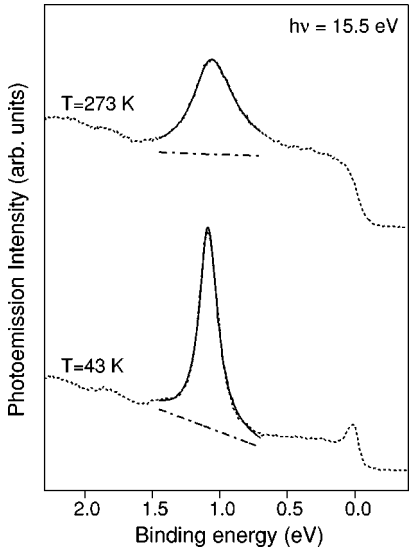

FIG. 6. The surface state is fitted with an asymmetric Lorentzian and a linear background in order to extract the linewidth. This is shown for a high- and a low-temperature spectrum.

asymmetry parameter of $\alpha = 0.04 \pm 0.02$. As indicated in the figure, the fit is performed only over a restricted region [1.45–0.7] eV including a linear background. This fitting procedure yields consistent fits for all temperatures and various photon energies. The absolute values for the widths depend on the specific choice of the line-shape function and the energy range to be fitted. However, the qualitative behavior of the lineshape versus temperature we report below is a robust and inherent feature independent of the fitting procedure.

The resulting linewidth for several measurements performed at 15.5 eV photon energy is shown in Fig. 7. In between each temperature scan the sample was cleaned. The most important observation is the almost sudden increase of linewidth at the temperature of the phase transition. The linewidth changes by over 100 meV in a temperature range of only 5 K. From this, the transition temperature can be determined to be 231 K. Below the phase transition the linewidth appears not to be a linear function of the linewidth. Rather, it is flattening out at the lowest temperatures. This behavior can be expected from Eq. (1) even in a simple Debye model. It is due to the ''freezing'' of the phonons at low temperatures.

From the included error bars one sees that the spread in data is somewhat larger than the uncertainty in the individual fits. This is most likely caused by the preparation history, e.g., the amount of surface defects. It is consistent with the fact that a much narrower distribution can be obtained by rigidly shifting the result from each temperature scan along the vertical axis. Such a rigid shift would be expected from the fact that the linewidth contributions are roughly additive, which has recently been verified experimentally.[26] We also notice that the relative spread is bigger in the HT phase.

Figure 7 also shows selected fits to the linewidth data below the phase transition. The changes close to the phase transition cannot be explained by the model given in Eqs. (1) and (2) and thus the region above 210 K has been excluded from the fitting region. Above the phase transition the temperature range it is too short to permit a meaningful fit. A linear fit, by Eq. (2), plus the temperature-independent offset Γ_0, has been performed for the region above $\Theta_D/3 \simeq 110$ K and from this we find $\Gamma_0 = 113 \pm 6$ meV and $\lambda_s = 1.01 \pm 0.06$. When trying to apply the full model, Eq. (1) plus offset, it turns out that the three free parameters λ_s, ω_D, and Γ_0 are highly correlated in the low-temperature region. We have therefore fixed the Debye temperature to the bulk value of α-Ga ($\omega_D = 28$ meV). In this case we find good agreement with the data and $\Gamma_0 = 88 \pm 3$ meV, $\lambda_s = 1.17 \pm 0.04$. This value of λ_s indicates a strong electron-phonon coupling in the surface,[30] even stronger than in the bulk.

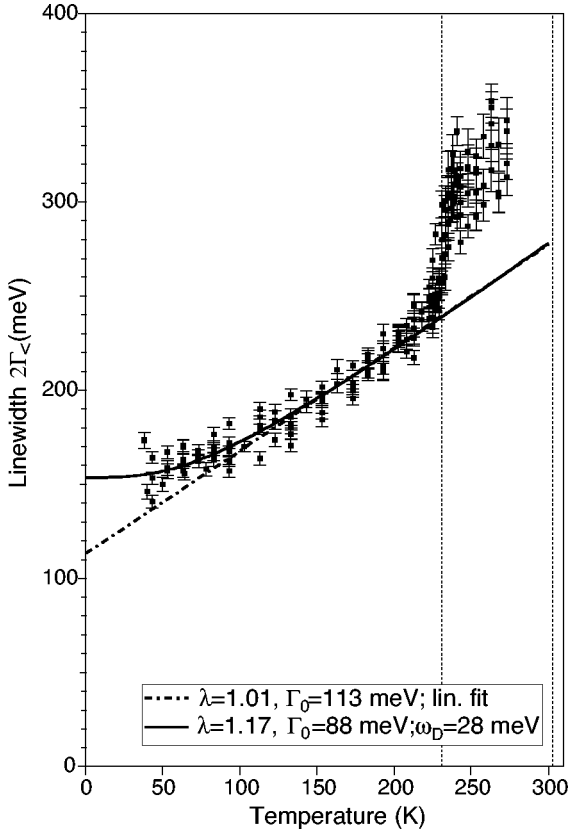

FIG. 7. Linewidth of the S_H state as a function of temperature. The data set consists of 11 independent series; the sample was cleaned before each series. The error bars represent the uncertainties resulting from the line-shape fitting procedure. In addition, a linear fit in the high-temperature limit [Eq. (2)] and a fit to the full model [Eq. (1)] with $\omega_D = 28$ meV are shown. The transition temperature $T_c = 231$ K and the melting point $T_m = 303$ K are marked by vertical lines.

The resulting fit parameters have to be viewed in light of the preparation dependence we have found for the linewidth and keeping in mind that a different fitting region for the determination of the Lorentzian width also leads to slightly different results. This is mostly affecting the temperature-independent offset and the absolute value of this parameter has to be treated with care. Note also that we did not choose to use the surface Debye temperature determined in the LEED study[10] because the meaning of this parameter is not entirely clear here. Nevertheless, the choice of the Debye

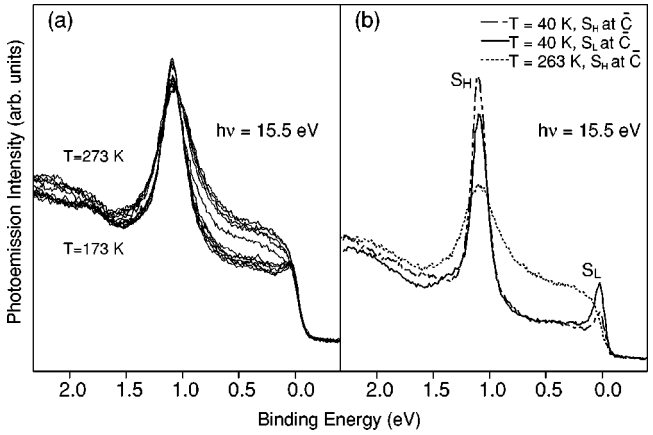

FIG. 8. (a) Spectra from the series shown in Fig. 5, plotted without vertical offset and in $\Delta T = 10$ K steps. A sudden change in the spectral shape at the temperature of the phase transition is easily recognizable. (b) Comparison between a high-temperature EDC and a low-temperature EDC for the S_H surface state at $\bar{C}$. Also shown is a low-temperature spectrum with the S_L surface state at $\bar{C}$. Notice how the S_L state increases the density of states at the Fermi level around $\bar{C}$.

temperature does have an influence on the other parameters due to the correlation in the fitting process, and the uncertainty in those parameters is thus larger than that suggested by the purely statistical errors.

In Fig. 8 we plot a set of EDC's taken at $\bar{C}$ in the vicinity of the phase transition without a vertical offset. Again one observes the narrowing of the S_H state upon decreasing temperature. More importantly, an apparently discontinuous change of the spectral form at the Fermi level and below is observed at the phase transition. Above the transition temperature merely a high Fermi edge is present. Just below, a small peak due to the S_L state is seen near the Fermi level, leading to an enhancement of spectral intensity there. Between the S_L state and the S_H state there is a considerable loss of spectral intensity. Note that this loss is intimately related to the sudden decrease of surface-state linewidth observed when cooling through the phase transition (see Fig. 7). The spectral intensity at binding energies higher than $\sim$1.8 eV does not seem to be affected much by the phase transition.

We summarize the main findings of this section. A reinvestigation of the temperature dependence of the S_H state confirms the presence of strong electron-phonon coupling as already reported by HCGB.[12] In a small energy range around the phase transition we observe a quasidiscontinuous change of spectral shape in the EDC's which is accompanied by a change in the linewidth of the S_H state. The S_L state is observed immediately below the transition temperature and seems to be characteristic for the LT phase, being completely absent above the transition temperature.

C. The electronic structure away from $\bar{C}$

When moving away from the $\bar{C}$ point, the S_H state shows a parabolic dispersion. The dispersion along two high-

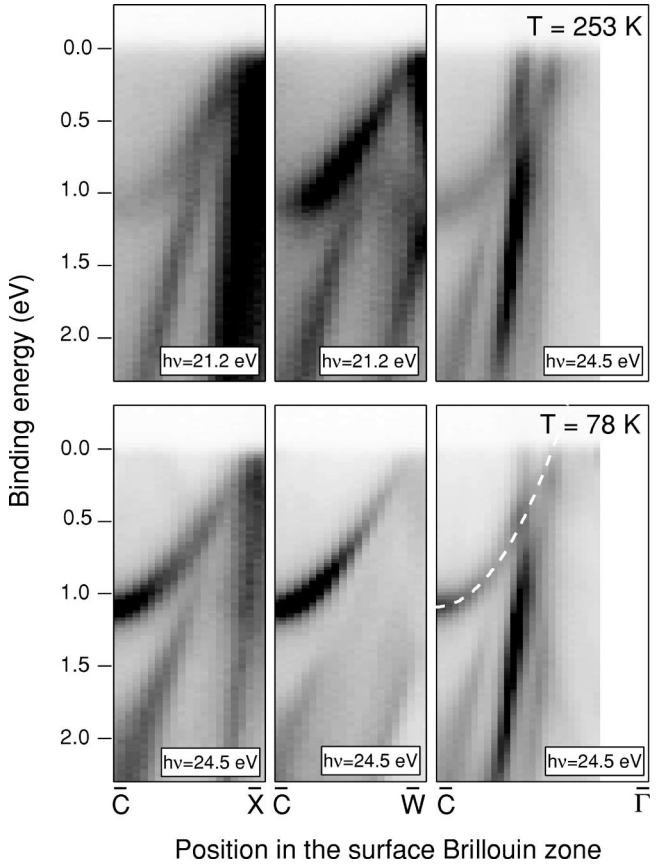

FIG. 9. Dispersion of the S_H state along selected high-symmetry directions away from the $\bar{C}$ point and for two temperatures above and below the phase-transition temperature. Black corresponds to high photoemission intensity. Note that some data are taken with a discharge lamp (21.2 eV) and some with synchrotron radiation (24.5 eV). The dashed white line in the right lower map is a free-electron parabola with an effective mass of 1.3 electron masses.

symmetry lines ($\bar{C}$-$\bar{X}$ and $\bar{C}$-$\bar{W}$) and along the $\bar{C}$-$\bar{\Gamma}$ line is shown in Fig. 9 for two temperatures, 253 K and 78 K. The dispersion around $\bar{C}$ was found to be well described by a free-electron parabola with an effective mass of 1.3 electron masses (also shown in Fig. 9). For the $\bar{C}$-$\bar{X}$ direction HCGB have observed a Fermi-level crossing of the quasiparticle peak in the HT phase. This crossing was removed in the LT phase. This simple scenario cannot be confirmed here. Our intensity pictures of data which were taken over a larger energy interval show clearly the presence of a strongly dispersing bulk feature which mixes with the surface state at about 0.5-eV binding energy. At lower binding energies, both features cannot be distinguished anymore. Close to the Fermi energy, both states form a broad peak which may have some spectral weight above the Fermi energy but does not show a clear crossing. At 78 K the state is sharper and the spectral weight at the Fermi level therefore smaller, but the qualitative dispersion in this region is similar. For $\bar{C}$-$\bar{W}$ we also see the strongly dispersing feature but it is unclear whether it mixes with the surface state. In both directions no clear Fermi-level crossing is observed in the HT phase but the S_L

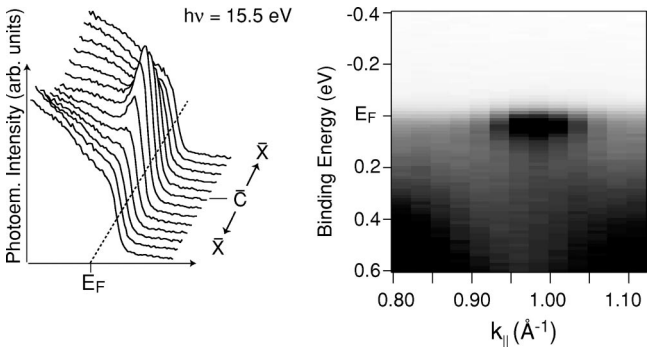

FIG. 10. Dispersion of the S_L state in the vicinity of $\bar{C}$, along the $\bar{C}$-$\bar{X}$ direction at $T=78$ K. The EDC's have been plotted with both vertical and horizontal offsets. Black corresponds to high photoemission intensity.

quasiparticle peak closely approaches the Fermi level. In the $\bar{C}$-$\bar{\Gamma}$ direction the situation is clearer. Here the surface-state dispersion ends in the bulk continuum about 400-meV below the Fermi level.

The S_L state is barely visible in the low-temperature data of Fig. 9 because its intensity with respect to S_H is relatively low; in addition to this the state is only present in a narrow range around $\bar{C}$. This can be seen in Fig. 10. When moving the emission angle away from $\bar{C}$, the S_L state appears to either cross the Fermi level or lose its intensity and disappear.

Figure 11 shows a set of spectra in the vicinity of the phase transition taken at an arbitrary point away from $\bar{C}$ (the point is indicated in Fig. 2). An observation similar to that in Fig. 8 is made: at the phase transition the spectral shape changes discontinuously. Away from $\bar{C}$, the S_L state is not present and consequently one finds a decrease of spectral intensity from the Fermi level down to the S_H state. There is

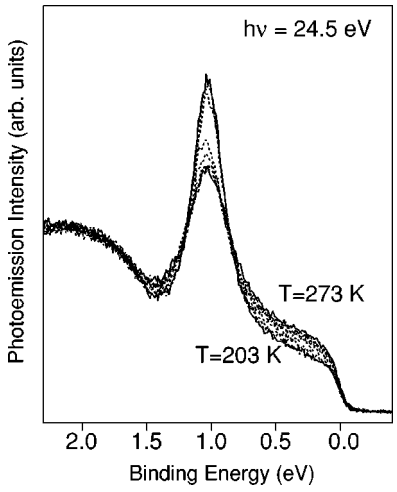

FIG. 11. Temperature-dependent ($\Delta T=10$ K) EDC's taken away from the $\bar{C}$ point on the $\vec{k}_{\|}$ point indicated in Fig. 2(b). At the temperature of the phase transition a sudden loss of spectral intensity is observed between the Fermi level and approximately 1.5-eV binding energy.

nothing special about this k point. We have performed such measurements at many other points in the projected band gap around $\bar{C}$ and made similar observations. A more systematic approach to this is described in the next subsection of the paper.

D. The two-dimensional Fermi surface

A discussion of the phase transition in terms of a CDW or, more general, a metal-insulator transition requires the experimental determination of the surface Fermi surface above and below the transition temperature. In the previous sections we have already seen that the phase transition leads to a quasi-discontinuous change of photoemission intensity at the Fermi level, at least at some points of the SBZ. The surface-state dispersions shown in Fig. 9 do not reveal any clear-cut Fermi surface in the directions considered but there may be some spectral intensity at E_F from the S_H state, or a surface resonance derived from this state, in both the $\bar{C}$-$\bar{X}$ and $\bar{C}$-$\bar{W}$ directions. In order to obtain more complete information about the surface Fermi surface in the entire SBZ, we have measured the photoemission intensity at the Fermi level for two photon energies (15.5 eV and 17 eV) and at two temperatures (273 K and 83 K). The intensity at the Fermi level was determined by integrating over a 50-meV energy window centered on the Fermi level. A background correction was performed by subtracting the averaged intensity of a 50-meV energy window well above the Fermi level. The mapping was only done in one irreducible quarter of the SBZ. The rest of the plots are obtained by symmetry. The resulting Fermi-level intensity maps are shown in Fig. 12. The color scale at each photon energy is chosen such that the same scaling applies to the HT and LT scans.

The strongest features in our maps of the Fermi-level intensity are the half circles close to $\bar{\Gamma}$ in the $\bar{\Gamma}$-$\bar{X}$ direction, the two horizontal features at the sides of the $\bar{X}$ point, and the pointlike feature at $\bar{W}$. All these are interpreted as bulk related. The peak at $\bar{W}$ must be a bulk feature or at least a surface resonance because there is no projected bulk band gap at $\bar{W}$.[13] All the other features are immediately identified as bulk related because one can see their form change with photon energy, demonstrating a sensitivity towards a change of $k_{\perp}$. For the HT phase, we do not observe a clear-cut surface Fermi surface caused by the Fermi-level crossing of the quasiparticle peak from the S_H state at any point of the SBZ. Instead, we find a relatively high intensity at the Fermi level in almost all of the projected bulk band gap around the $\bar{C}$ point. This intensity is much lower in the LT phase, consistent with Fig. 11. In the LT data the S_L state is visible as a relative maximum in intensity around $\bar{C}$, as expected. We do, however, also observe an increase of Fermi-level intensity in a broader region around $\bar{C}$ in the HT data, suggesting that the S_L state is still present to some degree but smeared out in k space, i.e., characteristic features of the LT structure are still present in a disordered way in the HT phase. This seems

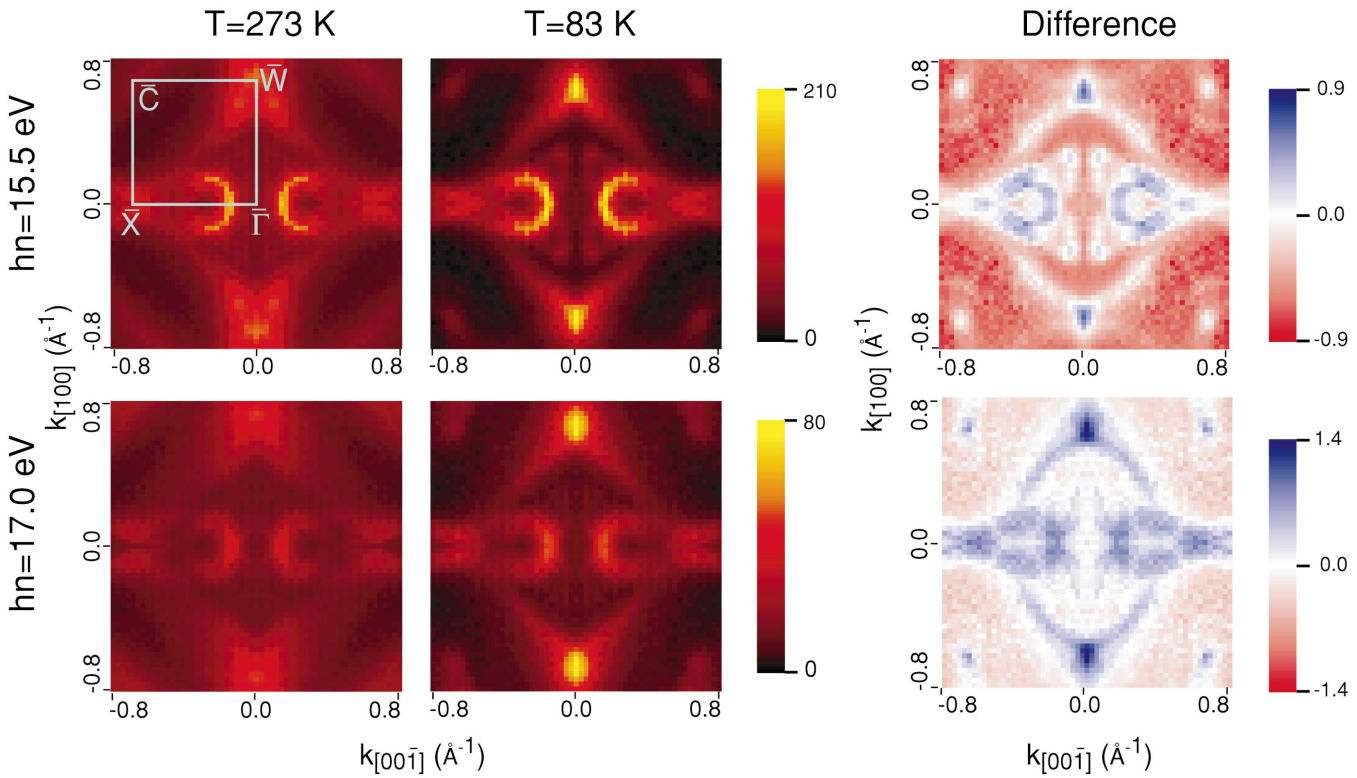

FIG. 12. (Color) Map of the integrated Fermi-level intensity at two different photon energies and temperatures. Data were only obtained in an irreducible quarter of the SBZ; the rest of the image was generated by symmetry. The difference is calculated as $(I_{LT}-I_{HT})/I_{HT}$.

surprising when only considering the data in Fig. 8 where the S_L state appears to be vanishing abruptly at the phase transition.

E. Core levels

Signs of the surface phase transition were also found in the shape of the Ga 3*d* core-level lines. The temperature dependence of the core-level spectra is shown in Fig. 13. Just as in the valence band, a sudden change of the core-level line shape is observed at the transition temperature. In the low-temperature phase the spin-orbit split components of the 3*d* line are apparently broadened as well as slightly shifted in energy. The line-shape change has some minor dependence on the emission angle as shown in Fig. 13. The changes related to the surface phase transition must obviously originate in a surface contribution to the 3*d* signal. The core-level binding energies of atoms in the surface layer may be different, by the so-called surface core-level shift (SCLS), from the bulk values. One could now imagine the SCLS to be different for the two phases, giving rise to the observed abrupt change in line shape. We have not been able to clearly identify SCLS components of the Ga 3*d* lines. In fact, spectra of the Ga 3*d* line for various emission angles and photon energies are generally quite well fitted with two Gaussian broadened Doniach-Sunjic line shapes. The fit parameters were Gaussian width 290 meV (HT) and 340 meV (LT), Lorentzian width 180 meV, and asymmetry parameter 0.05. Note that the Gaussian broadening is an intrinsic effect due to phonon scattering of the core hole, and it is significantly greater than the instrumental broadening. The fact that we are not able to resolve any SCLS components does not rule out this explanation of the line-shape change. The angular dependence seen in Fig. 13 is most likely due to different photoelectron-diffraction effects for the surface and the bulk components.

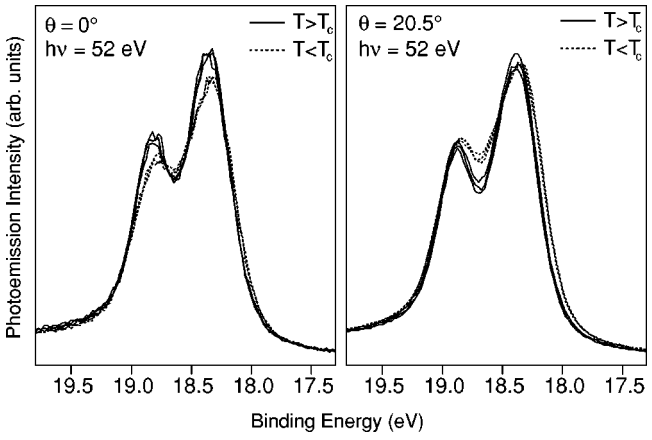

FIG. 13. Temperature dependence of Ga 3*d* for two different polar emission angles (θ). The spectra are taken in $\Delta T=10$ K steps between 203 K and 253 K.

Related to the SCLS difference between the surface and bulk, one may also consider whether the Ga 3*d* states show some band-structure behavior. The 3*d* states are shallow and may not be fully localized. If this is the case, the surface band structure would be expected to be different from that of the bulk. Our observation could then be explained by a

change in the $3d$ surface band structure at the phase transition. We have investigated the possibility of band dispersion in the $3d$ states by looking at the angular dependence of the line shape. Such a dependence was not found.

IV. DISCUSSION

Several ingredients seem to be important in the phase transition: an at least partial dimerization of the surface atoms,[10] a loss of spectral intensity near the Fermi level in a large fraction of the SBZ, the absence of a clear-cut nested Fermi surface from the S_H state quasiparticle peak, a partially disordered HT phase which resembles the LT phase, and probably also the strong electron-phonon coupling. All these points lead us to interpret the transition tentatively as a scenario which was termed a ''strong-coupling CDW'' by Tosatti.[16] In this case the HT phase is governed by the same short-range order as the LT phase, only the long-range order is lost. Just above the transition temperature the local structure and electronic structure will be very similar to that of the LT structure but governed by strong fluctuations.[18] It is important to point out that in this case the HT structure is most adequately described in a short-range real-space picture, not in k space where all the structures will be smeared out. Only at a much higher temperature, above the melting temperature of the sample, also the short-range ordering is undone and the sample can be described again as an ordered solid in k space. In the following, we give a detailed discussion of our findings in light of this picture.

A. Surface Fermi surface

The most important result of our Fermi-surface scans is that the HT to LT transition is accompanied by a decrease of spectral intensity at the Fermi level in a large fraction of the projected band gap around $\bar{C}$. At the same time we fail to observe a nested Fermi surface in the HT phase. We show that these results are consistent with the strong-coupling CDW picture.

In order to discuss the possibility of Fermi-surface nesting, it is useful to have two limiting cases of the structure in mind. The first is to view the reconstruction, crudely simplified, as $(\sqrt{2}\times\sqrt{2})R45°$. In this case one would have to look for a Fermi surface with a nesting vector corresponding to the $\bar{\Gamma}$-$\bar{C}$ vector. The S_H surface state would be a good candidate to set up such a nesting. It would have to have Fermi-level crossings half way along the $\bar{\Gamma}$-$\bar{C}$ line. In addition to this, the Fermi surface should continue as straight lines perpendicular to the $\bar{\Gamma}$-$\bar{C}$ line. The other limiting case is the complicated real structure which is not only $(2\sqrt{2}\times\sqrt{2})R45°$ but also shows split spots in SPA-LEED which indicate a periodicity about 18 times the lattice constant in the direction of the glide plane. In this structure, Fermi-surface nesting could happen almost over the entire (1×1) Brillouin zone where the S_H state crosses the Fermi level.

It turns out, however, that both the surface-state dispersion in Fig. 9 and the Fermi-level intensity scans in Fig. 12 do not show any clear surface Fermi-level crossings, neither in the $\bar{\Gamma}$-$\bar{C}$ direction nor anywhere else. Instead we observe a smeared out Fermi-level intensity in the HT phase which disappears in the low-temperature phase not only along $\bar{\Gamma}$-$\bar{C}$ but in a large fraction of the projected bulk band gap around $\bar{C}$. The absence of a well-defined Fermi surface for the HT phase is particularly striking when we compare our data to the theory of BCT for the B termination which we assume to be the correct structure for the HT phase. According to BCT, the S_H surface state should have an almost circular Fermi surface around the $\bar{C}$ point and a maximum binding energy of about 0.5 eV. Our findings reveal no clear Fermi surface and a maximum binding energy of 1.1 eV. One could be tempted to argue that the absence of the Fermi surface is related to the higher binding energy at the $\bar{C}$ point which shifts the whole surface-state dispersion down and causes the bands to end up in the bulk continuum rather than cross the Fermi surface. But the problem lies deeper than this. The S_H state on the B termination is a dangling-bond state and thus only partly occupied. This means that it has to have a Fermi surface.

This apparent problem is solved by considering the importance of fluctuations in the HT phase which destroy the long-range order present in the LT phase. These fluctuations will necessarily lead to a situation where the information gathered in photoemission is unclear. In simple terms this is due to the fact that $k_\parallel$ is not a good quantum number anymore and one cannot expect to measure a well-defined two-dimensional Fermi surface. Our findings for the spectral changes near the Fermi level which accompany the phase transition fit very well into this picture: In most regions of the SBZ this change is a loss of spectral intensity. Directly at $\bar{C}$ this is not the case. The intensity at the Fermi level changes only very little because of the S_L state's appearance below the transition temperature. The change of spectral intensity is not restricted to the immediate vicinity of the Fermi level. In fact, Fig. 11 shows a loss of spectral intensity all the way from the Fermi level to the surface-state peak where one observes an intensity increase. At binding energies higher than 1.8 eV or so the phase transition does not seem to have a major influence on the spectral features, neither off nor at $\bar{C}$. The entire behavior can be interpreted as the removal of an ill-defined Fermi surface, as expected for a strong-coupling CDW. Note that the spectroscopic signatures of our phase transition are very similar to the findings of Dardel *et al.* for the incommensurate to quasicommensurate transition on $1T$-TaS_2.[27] In that system one observes the sudden opening of a pseudogap together with spectral changes over an energy range much larger than the kT associated with the phase transition.

B. Electron-phonon coupling and lifetime effects

The present study has confirmed the fact that the electron-phonon coupling is very strong on α-Ga(010), a fact that would favor the type of phonon-softening transition we have in mind. The sudden increase of linewidth of the S_H state at the phase-transition temperature, however, cannot be explained in the usual picture of lifetime effects. Indeed, one

could expect a jump *in the other direction* when considering the fact that the low-temperature structure is reconstructed. This is because the reconstruction provides smaller reciprocal-lattice vectors which couple the S_H state to other electronic states, potentially reducing the lifetime. A possible explanation for the observed linewidth increase in the HT phase is that a new decay channel, which could but does not have to be a phonon, is opened at the phase transition. Such a channel could be the coupling to structural fluctuations still present in the HT phase. An alternative explanation is the fact that $k_\parallel$ ceases to be a good quantum number in the HT phase. The transition from the LT to the HT phase is accompanied by a $k_\parallel$ smearing. This leads to a broadening of the surface state not because of a new decay channel for the hole but simply because the initial state is not well defined anymore in $k_\parallel$. In this case, however, one would expect an asymmetric broadening of the S_H state towards lower binding energies which was not found in our analysis of the peak shape.

In a strong-coupling CDW scenario, the above considerations would also apply, to a small degree, to the LT phase. At finite temperatures, a CDW state is not perfectly ordered either. An interaction between the excitations of the CDW state and the electronic states will at least contribute to the finite background intensity below the Fermi level and to the surface-state linewidth. This effect has to also to be kept in mind when linking a strong temperature dependence of the surface state width below the transition temperature exclusively to electron-phonon coupling. However, at very low temperatures this should be unimportant and we must clearly state that the reason for the relatively high background intensity below the Fermi level is not yet understood.

C. Similarity between HT and LT phases: The S_L state

There are indications pointing towards a close similarity between the HT and the LT phases which would be expected for the strong coupling CDW model. From the temperature scans of the S_L state peak at $\overline{C}$ it appears that this feature is closely linked to the phase transition and genuinely belongs to the LT phase. Our Fermi-level intensity scans show, however, that a higher but smeared out Fermi-level intensity around $\overline{C}$, reminiscent of the peak caused by the S_L state, can also be found above the transition temperature. This change from a sharp peak (in $k_\parallel$) to a broad maximum is consistent with a strong-coupling CDW model which only destroys the long-range order and therefore leads to a $k_\parallel$ smearing in the HT phase.

The problem is that we have little knowledge of the significance of the S_L state in the first place since we are lacking theoretical calculations of the electronic structure in the LT phase. When viewing the reconstruction as ''almost'' $(\sqrt{2}\times\sqrt{2})R45°$ one could expect an umklapp process which folds the states from the $\overline{\Gamma}$ point into the $\overline{C}$ point, and the S_L state could be the same as the surface state at $\overline{\Gamma}$ shown in Fig. 3. This origin of the S_L state can, however, be excluded because it is much closer to the Fermi level than the state at $\overline{\Gamma}$. Another possibility is that the S_L state is simply a band which lies just above the Fermi level for the HT phase and is pulled down by the reconstruction. This seems rather unlikely, too. When we view the LT structure as a slight distortion of the HT phase, a state above the Fermi energy at $\overline{C}$ should be found in the calculations of the electronic structure of the B termination but this is not the case.[13] It seems more likely that the S_L peak has a more complicated many-body nature which is linked to the LT phase. It could originate from low-lying excitations of the CDW state. More theoretical work is needed to resolve this issue.

D. Core levels

We have observed signs of the phase transitions not only in the valence band but also in the $3d$ core-level spectrum. It leads to an apparent broadening of the peaks when cooling from the HT phase to the LT phase. Unfortunately, the effect is rather small and we have not been able to pin down its origin, neither with data taken at different emission directions nor at different photon energies. In any event, a broadening in the low-temperature phase is counterintuitive. If surface core-level shifts play a role, one would expect them to be smaller in the LT phase because of the tendency of the surface to form dimers. If the $3d$ states are bandlike, a $k_\parallel$ smearing in the HT phase would predict broader peaks there, not in the LT phase. The only possible explanation was already given when discussing the S_H state. In the LT phase the new and small reciprocal-lattice vectors could couple different $k_\parallel$ points giving rise to a partial SBZ integration and broader lines. This speculation does not get us very far, however. What we do learn from the $3d$ states is that it might be important to include them as valence states in a future calculations of the α-Ga(010) surface properties.

E. Other issues

The presence of large thermal fluctuations in the HT phase agrees well with an increased surface disorder at the phase transition observed by SPA-LEED,[11] and with the fact that good agreement between simulated and measured LEED $I(V)$ curves for the HT phase can only be achieved using a very low surface Debye temperature in the simulations.[10] Note that the concept of the surface Debye temperature in a quantitative LEED analysis is intended to describe the enhanced thermal vibrations at the surface. Other kinds of disorder will, however, also result in the need to assume a low Debye temperature for the LEED simulations. On the other hand, the LEED analysis of the LT data also requires the assumption of a low Debye temperature. This leaves the possibility that the surface vibrational amplitudes are indeed very large.

The LEED results suggest, in agreement with naive intuition, that a dimerization in the surface does at least play some role in driving the phase transition. Such a dimerization should remove the dangling bonds and decrease the metallicity of the surface. In other words, one should observe a decrease in the density of states at the Fermi level in the LT phase or, in a pure band picture, the removal (partly) of the surface Fermi surface.

In connection to the discussion of CDW phenomena it is interesting to point out that (bulk) α-Ga can be viewed, in a certain sense, as a layered material where metallic planes, the buckled planes, are separated by covalent bonds. This point of view agrees with the very anisotropic Fermi surface and transport properties of α-Ga. In this picture, a B-terminated (010) surface is a quasi-two-dimensional metal. It should be even more metallic than the corresponding bulk layers due to the dangling bonds. It is a curious fact that this increased metallicity apparently leads to an unstable situation and a phase transition which is not observed in the bulk buckled planes.

V. CONCLUSIONS

We have studied the interplay between the surface phase transition and the electronic structure on α-Ga(010). Our findings lead us to an interpretation of the transition in terms of a surface charge-density wave. The most important facts to support this are the loss of spectral intensity at the Fermi level in large fractions of the SBZ, the strong electron-phonon coupling, and the presence of disorder in the high-temperature state. This disorder is most probably due to the fact that the short-range surface structure in the high-temperature phase still resembles the low-temperature phase but the long-range order is lost.

There are several open questions which call for further experiments and calculations. First of all, it would be desirable to measure the surface vibrational structure by electron energy-los spectroscopy or He scattering in order to learn more about the role of the surface phonons in the phase transition. Furthermore, knowing more details about the long-range order in the low-temperature structure would be important. LEED or x-ray scattering are probably not options here and low-temperature STM seems to be the only possible alternative. Last but not least, first-principles calculations of the low-temperature structure and electronic structure, at least for a $(\sqrt{2}\times\sqrt{2})R45°$ phase or maybe even for $(2\sqrt{2}\times\sqrt{2})R45°$, would be most valuable.

ACKNOWLEDGMENTS

We gratefully acknowledge many stimulating discussions about α-Ga with E. Tosatti, G. Chiarotti, and M. Bernasconi. This work has been supported by the Danish National Research Council and the Carlsberg Foundation. H. Li thanks the Danish Foreign Ministry for a DANIDA fellowship.

[1] R. W. G. Wyckoff, *Crystal Structures* (Interscience, New York, 1963).
[2] M. Bernasconi, G. L. Chiarotti, and E. Tosatti, Phys. Rev. B **52**, 9988 (1995).
[3] Ch. Søndergaard, Ch. Schultz, S. Agergaard, S. V. Hoffmann, Z. Li, Ph. Hofmann, H. Li, Ch. Grütter, and J. H. Bilgram, Phys. Rev. B (to be published).
[4] W. B. Waeber, J. Phys. C **2**, 903 (1969).
[5] G. Grimvall, *The Electron-Phonon Interaction in Metals* (North-Holland, Amsterdam, 1981).
[6] R. Trittibach, Ch. Grütter, and J. H. Bilgram, Phys. Rev. B **50**, 2529 (1994).
[7] O. Züger and U. Dürig, Phys. Rev. B **46**, 7319 (1992).
[8] O. Züger and U. Dürig, Ultramicroscopy **42-44**, 520 (1992).
[9] D. A. Walko, I. K. Robinson, Ch. Grütter, and J. H. Bilgram, Phys. Rev. Lett. **81**, 626 (1998).
[10] S. Moré, E. Soares, M. A. van Hove, Ph. Hofmann, S. Lizzit, A. Baraldi, Ch. Grütter and J. H. Bilgram (unpublished).
[11] S. Lizzit, A. Baraldi, Ph. Hofmann, Ch. Grütter and J. H. Bilgram (unpublished).
[12] P. Hofmann, Y. Q. Cai, Ch. Grütter, and J. H. Bilgram, Phys. Rev. Lett. **81**, 1670 (1998).
[13] M. Bernasconi, G. L. Chiarotti, and E. Tosatti, Phys. Rev. Lett. **70**, 3295 (1993); M. Bernasconi, G. L. Chiarotti, and E. Tosatti, Phys. Rev. B **52**, 9999 (1995).
[14] M. Bernasconi, Ph.D. thesis, International School for Advanced Studies (ISAS), Trieste, 1993.
[15] G. Grüner, *Density Waves in Solids*, Vol. 89 of *Frontiers in Physics* (Persus, Cambridge, MA, 1994).
[16] E. Tosatti, in *Electronic Surface and Interface States on Metallic Systems*, edited by E. Bertel and M. Donath (World Scientific, Singapore, 1995), and references therein.
[17] T. Aruga, J. Phys.: Condens. Matter **14**, 8393 (2002), and references therein.
[18] W. L. McMillan, Phys. Rev. B **16**, 643 (1977).
[19] J. E. Inglesfield, J. Phys. C **12**, 149 (1979).
[20] S. V. Hoffmann, Ch. Søndergaard, Ch. Schultz, Z. Li, and Ph. Hofmann (unpublished).
[21] Ch. Søndergaard, Ph.D. thesis, University of Aarhus, 2001.
[22] B. A. McDougall, T. Balasubramanian, and E. Jensen, Phys. Rev. B **51**, 13 891 (1995).
[23] J. Kliewer, R. Berndt, E. V. Chulkov, V. M. Silkin, P. M. Echenique, and S. Crampin, Science **288**, 1399 (2000).
[24] N. V. Smith, Comments Condens. Matter Phys. **15**, 263 (1992).
[25] N. V. Smith, P. Thiry, and Y. Petroff, Phys. Rev. B **47**, 15 476 (1993).
[26] L. Perfetti, C. Rojas, A. Reginelli, L. Gavioli, H. Berger, G. Margaritondo, M. Grioni, R. Gaál, L. Rorró, and F. R. Albenque, Phys. Rev. B **64**, 115102 (2001).
[27] B. Dardel, M. Grioni, D. Malterre, P. Weibel, Y. Baer, and F. Lévy, Phys. Rev. B **45**, 1462 (1992); B. Dardel, M. Grioni, D. Malterre, P. Weibel, Y. Baer, and F. Lévy, *ibid.* **46**, 7407 (1992).
[28] Note that there are different conventions in use for the crystallographic directions in α-Ga. We and Refs. 12 and 9 follow the crystallographic convention ($Cmca$ symmetry) while Refs. 7,8,13 and 14 follow the historic (pseudotetragonal) convention. In the latter case the b and $\bar{c}$ axes are reversed and the structure has the nonstandard $Mbab$ symmetry. Our (010) surface corresponds to the (001) surface in this case.
[29] The sample needs to be well aligned since the missing spots are only observed in normal-incidence LEED; if the LEED apparatus used by Züger and Dürig was not perfectly aligned this could

explain the discrepancy with the other LEED experiments.

[30] The value of λ_s determined here is similar to the result of HCGB although the absolute linewidth values in that work were smaller and the fit was performed with the unlikely assumption of no temperature-independent broadening. Note that our approach to data analysis is different from that pursued by HCGB where the fitting of the peaks was done with a Voigt line, assuming a certain energy resolution. Our energy resolution is much smaller than the peak width such that only a fit with a Lorentzian is required, i.e., we neglect any Gaussian broadening.